International Journal of Bifurcation and Chaos, Vol. 7, No. 3 (1997) 707–720

CHAOS IN ROBOT CONTROL EQUATIONS

SHRINIVAS LANKALAPALLI and ASHITAVA GHOSAL*
Robotics & CAD Laboratory, Department of Mechanical Engineering, Indian Institute of Science, Bangalore 560 012, India

Received April 22, 1996; Revised August 2, 1996

The motion of a feedback controlled robot can be described by a set of nonlinear ordinary differential equations. In this paper, we examine the system of two second-order, nonlinear ordinary differential equations which model a simple two-degree-of-freedom planar robot, undergoing repetitive motion in a plane in the absence of gravity, and under two well-known robot controllers, namely a proportional and derivative controller and a model-based controller. We show that these differential equations exhibit chaotic behavior for certain ranges of the proportional and derivative gains of the controller and for certain values of a parameter which quantifies the mismatch between the model and the actual robot. The system of nonlinear equations are non-autonomous and the phase space is four-dimensional. Hence, it is difficult to obtain significant analytical results. In this paper, we use the Lyapunov exponent to test for chaos and present numerically obtained chaos maps giving ranges of gains and mismatch parameters which result in chaotic motions. We also present plots of the chaotic attractor and bifurcation diagrams for certain values of the gains and mismatch parameters. From the bifurcation diagrams, it appears that the route to chaos is through period doubling.

1. Introduction

The two-degree-of-freedom planar robot, shown in Fig. 1, is the simplest possible robot. It consists of two rigid links and two rotary or revolute (R) joints, with the first link attached to the ground through an R joint and attached to the second link through the second R joint. Motors and sensors (such as optical encoders) are provided at the joints to drive the links through desired angles and for feedback control. For the two-link robot shown in Fig. 1, by appropriately actuating the joints, we can position the tip of the second link (also called the end-effector) at any arbitrary Cartesian position inside its workspace. The relationships between the joint variables, (θ_1, θ_2), and the Cartesian variables, (x, y) can be easily obtained for this simple robot. It may be mentioned that a general six-degree-of-freedom robot which can arbitrarily position and orient its end-effector in three-dimensional space has six actuated joints and for such robots the relationship between the joint variables and the Cartesian variables is vastly more complicated (see Craig, 1989).

The task to be performed by a robot can involve moving the end-effector from one point to another (point to point motion) or moving the end-effector along a desired trajectory (trajectory tracking). The control problem for robots is that of determining the time history of motor torques required to cause the end-effector to execute a desired motion. A control algorithm is required for this purpose and there exist a number of them. One

*E-mail: asitava@mecheng.iisc.ernet.in

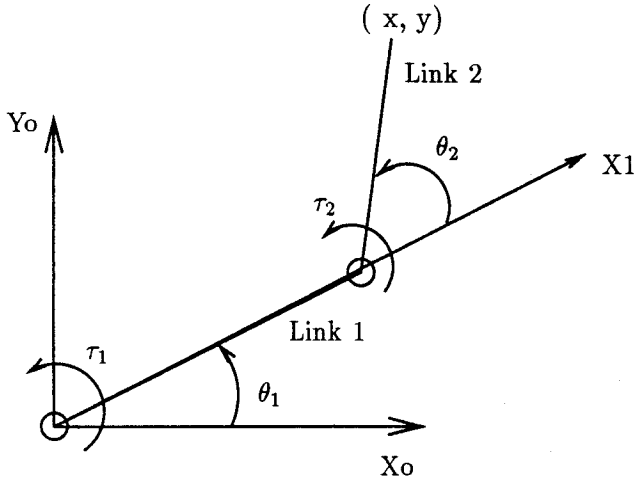

Fig. 1. A schematic of a 2R planar rigid robot.

of the most common control algorithm is the independent joint proportional plus derivative (or PD) control where the motor torque is proportional to the error (desired joint rotation minus the measured joint rotation) and to the rate of change of error.[1] Another control algorithm uses the dynamic model of the robot together with the error driven portion (see Sec. 2 for details). These control algorithms have been studied extensively and implemented on actual robots. Studies show that a robot operating under the above two control algorithms is stable for point to point and trajectory tracking under certain conditions on the controller gains and estimates of the model [Asada & Slotline, 1986; Spong & Vidyasagar, 1989; Craig, 1988]. It is also claimed that these control algorithms are robust to changes in controller gains [Asada & Slotline, 1986] and model parameters [Craig, 1988].

In this paper, we take a second look at the control problem for robots, in particular the simplest two-link robot shown in Fig. 1, undergoing repetitive motions in the Cartesian space. We show that the nonlinear, ordinary differential equations, which describe the motion of a robot under PD or model-based control, can exhibit chaos for certain ranges of controller gains and for large mismatch in model parameters. This issue of possible chaotic motions has not been addressed in depth by researchers in the area of robust control of robots.

The organization of the paper is as follows: In the rest of this section, we present some of the relevant literature and discuss the points of difference with the vast existing literature on chaotic motions. In Sec. 2, we present the dynamics and control equations for the two-link robot under consideration. In Sec. 3, we present the numerical techniques used in this study followed by the numerical results and discussion in Sec. 4. Finally, in Sec. 5, we present the conclusions.

1.1. *Literature review*

There exists a large amount of work on chaos in mechanical and electrical systems. Moon in his book [1987] provides a list of the many phenomena where chaos has been observed in these systems. However, there are very few works on chaos in robots reported in literature. Vakakis and Burdick [1992] and M'Closeky and Burdick [1993] have studied periodic and chaotic motions in the dynamics of a simplified hopping robot. In this study, the leg of the hopping robot is modeled as a nonlinear spring whose restoring force is inversely proportional to the displacement. Buhler and Koditschek [1990, 1991] have studied a simplified model of a planar juggling robot. The task of robot juggling involves intermittent robot-environment interactions which give rise to nonlinear maps. Mahout *et al.* [1992a] have done a numerical study of the equations of motion of a 2R robot with periodic joint torques. They have observed chaotic motions for certain robot parameters. In another work [Mahout *et al.*, 1992b], they have reported subharmonic, fractional harmonic and chaotic motion in the equations of a 2R robot under PD control for certain values of the gains of the controller. Streit *et al.* [1986, 1988, 1989] have studied the equations of motion of a two-degree-of-freedom flexible manipulator with a prismatic (sliding) joint and a revolute joint performing repetitive tasks. They show that the flexible variables can undergo period-doubling bifurcations leading to chaos.

A two-link robot moving in the *vertical plane* can also be considered as a driven double pendulum. The passive double pendulum is one of the classic paradigms of a physical system exhibiting chaos. Chaos has been demonstrated both by experiments and numerical simulations [Levien & Tan, 1993;

[1]Often, a term proportional to the integral of the error is also added, and these are called PID controllers.

Richter & Scholz; Shinbrot *et al.*, 1992] in the double pendulum. Except for the work of Dullin [1994], to our knowledge, there exists no other analytical work on chaos in the double pendulum system. There is, however, a major difference between the two-link feedback controlled robot studied in this paper and the double pendulum. In the equations of the robot moving in the *horizontal plane*, there are no gravity terms and hence we do not have the stable and unstable equilibrium positions typical of pendulum systems. We will see later that for the two-link robot the only fixed point is the origin.

2. Dynamics and Control of a Two-Link Robot

Figure 1 shows a schematic of the two-link robot under consideration. The robot consists of two links of length l_1 and l_2 which move in the horizontal plane. The rotations at the two rotary (R) joints are denoted by θ_1 and θ_2 and the motion of the end-effector of the robot in Cartesian space is denoted by (x, y). The dynamic equations of the system can be derived using the Lagrangian formulation [Craig, 1989]. For the two-link robot, the equations of motion can be written as

$$\begin{aligned}&[m_1 r_1^2 + I_1 + I_2 + m_2 r_2^2 + m_2 l_1^2 + 2m_2 l_1 r_2 \cos(\theta_2)]\ddot{\theta}_1 \\ &\quad + [m_2 r_2^2 + I_2 + m_2 l_1 r_2 \cos(\theta_2)]\ddot{\theta}_2 - m_2 l_1 r_2 \sin(\theta_2)[2\dot{\theta}_1 + \dot{\theta}_2]\dot{\theta}_2 = \tau_1 \\ &[m_2 r_2^2 + I_2 + m_2 l_1 r_2 \cos(\theta_2)]\ddot{\theta}_1 + [m_2 r_2^2 + I_2]\ddot{\theta}_2 + m_2 l_1 r_2 \sin(\theta_2)\dot{\theta}_1^2 = \tau_2\end{aligned} \tag{1}$$

where, m_i, l_i, I_i and r_i are the mass, length, inertia and position of the center of mass of link i respectively, and τ_1, τ_2 are the actuating torques at the two joints. Equation (1) can be written in matrix form as:

$$\mathbf{M}(\boldsymbol{\theta})\ddot{\boldsymbol{\theta}} + \mathbf{C}(\boldsymbol{\theta}, \dot{\boldsymbol{\theta}}) = \Gamma \tag{2}$$

where, $\boldsymbol{\theta}(t)$ is the 2×1 vector of joint angles, $\mathbf{M}(\boldsymbol{\theta})$ is the 2×2 symmetric and positive definite mass matrix, $\mathbf{C}(\boldsymbol{\theta}, \dot{\boldsymbol{\theta}})$ is the 2×1 vector of Coriolis and centrifugal torques and Γ is the 2×1 vector of joint torques.

We assume the robot to be instrumented with sensors at each joint to measure the joint angle, and a motor at each joint to apply a desired torque on the neighboring link. In order to move the end-effector from one point to another or to track a desired path in the Cartesian space (the horizontal plane) the joints must be rotated through appropriate angles in the joint space (space formed by joint variables). This requires the motors to be commanded in a continuous manner and necessitates the use of some kind of a control system to compute the appropriate motor commands which will realize a desired motion. There exist a number of control schemes and these range from the simple *independent joint control* to the more sophisticated *model-based control* [Craig, 1989]. We first describe the *independent joint control scheme* and then the model based control scheme.

2.1. *Independent joint control*

In the independent joint control scheme, the joint torques are computed as

$$\Gamma = \ddot{\boldsymbol{\theta}}_d + K_v \dot{E} + K_p E \tag{3}$$

where $E = \boldsymbol{\theta}_d - \boldsymbol{\theta}$ is the servo error, and $\dot{E}$ is the derivative of the servo error.

The above control scheme is also called the proportional and derivative (PD) control scheme, and often a term which is proportional to the integral of the error is added for reducing steady state errors. This scheme can be proved to be asymptotically stable [Asada & Slotline, 1986] for any positive velocity gain ($K_v > 0$) for a regulator or set point tracking problem ($\dot{\theta}_d = \ddot{\theta}_d = 0$). However, such results do not exist for the robot joint trajectory tracking problem ($\dot{\theta}_d \neq 0$ and $\ddot{\theta}_d \neq 0$). In this control scheme, each joint is controlled as a separate control system without taking into account any of the dynamic coupling between the joints. In contrast, the model-based control scheme, described next, incorporates a complete dynamics model of the system in the computation of the actuation torques.

2.2. *Model based control*

In the *model-based control* scheme the joint torque is composed of two parts. One part is computed based on the supposed knowledge of the parameters

of the robot and is called the *model-based* portion of the control law. The second part is computed in a manner similar to the independent joint control and is called the *servo portion* of the control law. The torque computed by the control law is represented as

$$\Gamma = \hat{\mathbf{M}}(\boldsymbol{\theta})\Gamma_p + \hat{\mathbf{C}}(\dot{\boldsymbol{\theta}}, \boldsymbol{\theta}) \tag{4}$$

where, $\hat{\mathbf{M}}(\boldsymbol{\theta})$ is the estimated mass matrix of the original system, $\hat{\mathbf{C}}(\dot{\boldsymbol{\theta}}, \boldsymbol{\theta})$ is the estimated Coriolis and centripetal torques vector, and

$$\Gamma_p = \ddot{\boldsymbol{\theta}}_d + K_v\dot{E} + K_pE \tag{5}$$

is the servo law. In the above equation, K_p and K_v are positive definite diagonal gain matrices.

Substitution of Eqs. (5) and (4) into Eq. (2) results in the following closed loop system of equations.

$$\ddot{E} + K_v\dot{E} + K_pE = [\mathbf{M}(\boldsymbol{\theta}) - \hat{\mathbf{M}}(\boldsymbol{\theta})]\ddot{\boldsymbol{\theta}} + [\mathbf{C}(\dot{\boldsymbol{\theta}}, \boldsymbol{\theta}) - \hat{\mathbf{C}}(\dot{\boldsymbol{\theta}}, \boldsymbol{\theta})] \tag{6}$$

If the matrix $\hat{M}$ and vector $\hat{C}$ can be estimated exactly to be equal to the actual mass matrix M and Coriolis and centripetal torques vector C, then Eq. (6) reduces to

$$\ddot{E} + K_v\dot{E} + K_pE = 0 \tag{7}$$

The above equation is a set of uncoupled, linear second order differential equations, the eigenvalues of which will always lie in the left half plane for any positive gain matrices K_p and K_v. The system is asymptotically stable as $E \rightarrow 0$ as $t \rightarrow \infty$ and the actual trajectory $\boldsymbol{\theta}$ tracks the desired trajectory $\boldsymbol{\theta}_d$.

However, in practice, due to uncertainties in the system parameters, an exact model of the system cannot be obtained. The result is Eq. (6), which is a highly coupled system of nonlinear ordinary differential equations. It can be seen that the mismatch between the actual and the modeled parameters will cause servo errors to be excited according to the rather complicated Eq. (6) and stability is very difficult to conclude. Since an approximate model is used, robustness to parameter uncertainties is an important issue. Craig [1988] has proposed a conjecture which states that if the estimated mass matrix $\hat{M}(\boldsymbol{\theta})$ is positive definite and symmetric, and the velocity feedback is sufficiently large and positive, the system will be stable despite possibly large parameter errors. This conjecture is based on many simulations and trials on actual robots.

It may be noted that the independent joint or PD control scheme is a special case of model based control with $\hat{M}(\boldsymbol{\theta})$ taken as the identity matrix and $\hat{\mathbf{C}}(\dot{\boldsymbol{\theta}}, \boldsymbol{\theta})$ taken as zero.

3. State Space Robot Control Equations

We are interested in the global behavior of the closed-loop equations of the two control schemes to changes in feedback gains (K_p and K_v) and model uncertainties. The desired repetitive trajectories, in joint space, are assumed to be

$$\begin{aligned} \theta_{d1} &= A_1 \sin(\omega t) \\ \theta_{d2} &= A_2 \sin(\omega t) \end{aligned} \tag{8}$$

In the PD control scheme, the torques at the two joints are calculated as

$$\begin{aligned} \tau_1 &= \ddot{\theta}_{d_1} + k_{v_1}(\dot{\theta}_{d_1} - \dot{\theta}_1) + k_{p_1}(\theta_{d_1} - \theta_1) \\ \tau_2 &= \ddot{\theta}_{d_2} + k_{v_2}(\dot{\theta}_{d_2} - \dot{\theta}_2) + k_{p_2}(\theta_{d_2} - \theta_2) \end{aligned} \tag{9}$$

Substitution of Eq. (9) into Eq. (1) results in the closed-loop equations of the robot under PD control which can be represented in state space as

$$\begin{aligned} \dot{x}_1 &= x_2 \\ \dot{x}_2 &= (1/P_3(x_3))\{K_3(x_3)(K_2(x_3)x_2^2 + N_2(2x_2x_4 + x_4^2)) + N_2(\ddot{\theta}_{d_1} + k_{v_1}(\dot{\theta}_{d_1} - x_2) \\ &\quad + k_{p_1}(\theta_{d_1} - x_1)) - K_2(x_3)(\ddot{\theta}_{d_2} + k_{v_2}(\dot{\theta}_{d_2} - x_4) + k_{p_2}(\theta_{d_2} - x_3))\} \\ \dot{x}_3 &= x_4 \\ \dot{x}_4 &= (1/P_3(x_3))\{-K_3(x_3)(K_1(x_3)x_2^2 + K_2(x_3)(2x_2x_4 + x_4^2)) - K_2(x_3)(\ddot{\theta}_{d_1} + k_{v_1}(\dot{\theta}_{d_1} - x_2) \\ &\quad + k_{p_1}(\theta_{d_1} - x_1)) + K_1(x_3)(\ddot{\theta}_{d_2} + k_{v_2}(\dot{\theta}_{d_2} - x_4) + k_{p_2}(\theta_{d_2} - x_2))\} \end{aligned} \tag{10}$$

where, the state variables are defined as, $x_1 = \theta_1$, $x_2 = \dot{\theta}_1$, $x_3 = \theta_2$, $x_4 = \dot{\theta}_2$, and

$$\begin{aligned} P_3(x_3) &= \det[\mathbf{M}(x_3)] \\ K_1(x_3) &= m_1 r_1^2 + I_1 + I_2 + m_2 r_2^2 + m_2 l_1^2 + 2 m_2 l_1 r_2 \cos(x_3) \\ K_2(x_3) &= m_2 r_2^2 + I_2 + m_2 l_1 r_2 \cos(x_3) \\ K_3(x_3) &= m_2 l_1 r_2 \sin(x_3) \\ N_2 &= I_2 + m_2 r_2^2 \end{aligned} \tag{11}$$

In the model-based control scheme, we characterize the uncertainty in the model by a mismatch parameter ε. The estimated mass matrix $\hat{M}(\boldsymbol{\theta})$ and Coriolis and centripetal torques vector $\hat{C}(\boldsymbol{\theta}, \dot{\boldsymbol{\theta}})$ are computed by perturbing the robot parameters as follows:

$$\hat{m}_i = (1+\varepsilon) m_i\,, \quad \hat{r}_i = (1+\varepsilon) r_i\,, \quad \hat{I}_i = (1+\varepsilon) I_i\,, \quad \hat{l}_i = l_i \tag{12}$$

where, $\varepsilon > 0$ implies an overestimated model and $\varepsilon < 0$ implies an underestimated model. Since the mass matrix cannot be negative, $-1 < \varepsilon < \infty$. The joint torques are computed by Eq. (4).

Substitution of Eq. (4) into Eq. (1) result in equations of the robot under model-based control which can be represented in state space as

$$\begin{aligned} \dot{x}_1 &= x_2 \\ \dot{x}_2 &= (1/P_3(x_3))\{K_3(x_3)(K_2(x_3)x_2^2 + N_2(2x_2x_4 + x_4^2)) + N_2\{\hat{K}_1(x_3)\{\ddot{\theta}_{d_1} + k_{v_1}(\dot{\theta}_{d_1} - x_2) \\ &\quad + k_{p_1}(\theta_{d_1} - x_1)\} + \hat{K}_2(x_3)\{\ddot{\theta}_{d_2} + k_{v_2}(\dot{\theta}_{d_2} - x_4) + k_{p_2}(\theta_{d_2} - x_2)\} \\ &\quad - \hat{K}_3(x_3)(2x_2 + x_4)x_4\} - K_2(x_3)\{\hat{K}_2(x_3)\{\ddot{\theta}_{d_1} + k_{v_1}(\dot{\theta}_{d_1} - x_2) + k_{p_1}(\theta_{d_1} - x_1)\} \\ &\quad + \hat{N}_2\{\ddot{\theta}_{d_2} + k_{v_2}(\dot{\theta}_{d_2} - x_4) + k_{p_2}(\theta_{d_2} - x_2)\} - \hat{K}_3 x_2^2\}\} \\ \dot{x}_3 &= x_4 \\ \dot{x}_4 &= (1/P_3(x_3))\{-K_3(x_3)(K_1(x_3)x_2^2 + K_2(x_3)(2x_2x_4 + x_4^2)) - K_2(x_3)\{\hat{K}_1(x_3)\{\ddot{\theta}_{d_1} \\ &\quad + k_{v_1}(\dot{\theta}_{d_1} - x_2) + k_{p_1}(\theta_{d_1} - x_1)\} + \hat{K}_2(x_3)\{\ddot{\theta}_{d_2} + k_{v_2}(\dot{\theta}_{d_2} - x_4) + k_{p_2}(\theta_{d_2} - x_3)\} \\ &\quad - \hat{K}_3(x_3)(2x_2 + x_4)x_4\} + K_1(x_3)\{\hat{K}_2(x_3)\{\ddot{\theta}_{d_1} + k_{v_1}(\dot{\theta}_{d_1} - x_2) + k_{p_1}(\theta_{d_1} - x_1)\} \\ &\quad + \hat{N}_2\{\ddot{\theta}_{d_2} + k_{v_2}(\dot{\theta}_{d_2} - x_4) + k_{p_2}(\theta_{d_2} - x_3)\} - \hat{K}_3 x_2^2\}\} \end{aligned} \tag{13}$$

where, the state variables are defined as, $x_1 = \theta_1$, $x_2 = \dot{\theta}_1$, $x_3 = \theta_2$, $x_4 = \dot{\theta}_2$, and

$$\begin{aligned} \hat{K}_1(x_3) &= \hat{m}_1 \hat{r}_1^2 + \hat{I}_1 + \hat{I}_2 + \hat{m}_2 \hat{r}_2^2 + \hat{m}_2 \hat{l}_1^2 + 2 \hat{m}_2 \hat{l}_1 \hat{r}_2 \cos(x_3) \\ \hat{K}_2(x_3) &= \hat{m}_2 \hat{r}_2^2 + \hat{I}_2 + \hat{m}_2 \hat{l}_1 \hat{r}_2 \cos(x_3) \\ \hat{K}_3(x_3) &= \hat{m}_2 \hat{l}_1 \hat{r}_2 \sin(x_3) \\ \hat{N}_2 &= \hat{I}_2 + \hat{m}_2 \hat{r}_2^2 \end{aligned} \tag{14}$$

Equations (10) and (13) are systems of four first-order ordinary differential equations which are coupled, nonlinear and non-autonomous. The nonlinearity is in trigonometric and quadratic terms. In addition the systems are dissipative due to the presence of velocity feedback (terms multiplied by K_v). These dynamical systems are very much different from the many systems studied in literature. The absence of gravity eliminates the multiple fixed points typical of the pendulum and the double pendulum systems. The only fixed point is (0, 0, 0, 0). An analytical study appears difficult

from the complicated nature of the equations, but a numerical study is possible. In the next section, we present the details of the numerical study done for this system.

4. Numerical Study

To perform the numerical study we have chosen the physical parameters of an existing robot, the CMU Direct Drive Arm II [Khosla, 1986]. This is a six degree-of-freedom robot, in which all the joints are of direct drive construction, i.e. motors are mounted directly at the joints. The first two links of this robot move in the horizontal plane and we choose the parameters of these two links for the numerical study. The parameters are as follows:

Physical parameters

Link	Length (m)	Mass (kg)	C.G. (m)	Inertia (kgm^2)
1	0.5	20.15	0.18	6.3
2	0.4	8.25	0.26	1.64

As mentioned before we are interested in the global behavior when the mismatch parameter ε and controller gains K_p and K_v are varied. In general there would be four controller gains — k_{p_i} and k_{v_i} for each of the two joints. To reduce the number of parameters that can be varied, we have assumed that the gains are same for both joints. The desired repetitive trajectory (8) was assumed to have $A_1 = \pi/2$ rad, $A_2 = \pi/4$ rad, and $\omega = 2.0$ rad/s. The numerical integration was done by a variable step, variable order, predictor corrector Adams algorithm [Gordon & Shampine, 1975]. In order to ensure that the results were not an artifact of the numerical integration scheme, the solutions were verified with Runge-Kutta 5-6 [IMSL, 1989] integration routine. As an additional check the integration was done for relative and absolute error tolerances of 10^{-6} and 10^{-9}.

In the numerical study the following was done:

(a) *Time series and phase plots.*
Time series and phase plots were observed for different values of ε, K_p and K_v. These plots quickly give us an idea of the nature of the solution. Also the actual trajectory and the desired trajectory were plotted, to observe the performance of the controller.

(b) *Poincaré maps.*
The Poincaré map was obtained by sampling the solution at the forcing period (in our case π seconds). The computed map is in R^4 space and only projections in R^2 space were observed.

(c) *Lyapunov exponent.*
The Lyapunov exponent is a measure of the sensitivity of the system to changes in initial conditions. A positive exponent implies chaotic dynamics. All the Lyapunov exponents were computed using the algorithm of Wolf *et al.* [1985]. One of the Lyapunov exponents is zero since the system is periodically forced and non-autonomous. A search was done by systematically varying the gains K_p and K_v for different values of the mismatch parameter ε.

(d) *Bifurcation diagrams.*
The phenomenon of sudden change in the motion as a parameter is varied is called a bifurcation. A bifurcation diagram is a technique for examining the prechaotic (route to chaos) or post chaotic changes in a dynamical system under parameter variations. Bifurcation diagrams were computed using the brute force method [Parker & Chua, 1989] which essentially consists of varying the parameter in fixed steps and computing the Poincaré map for a finite number of periods at each step.

All the simulations were performed for different initial conditions and the same qualitative behavior was observed after neglecting the transients. We present below some of the many simulation results obtained by us.

5. Results and Discussion

We first demonstrate the performance of the controller for a good model and moderate gains. In this case ε has a small absolute value. Figure 2 shows the phase plots of the actual trajectory and the desired trajectory. It can be seen that the actual trajectory tracks the desired trajectory quite well. Figure 3 shows the phase plots with a model with $\varepsilon = -0.5$. It can be seen that the desired trajectory does not track the actual trajectory, but is periodic. A better performance can be obtained by increasing the values of the gains K_p and K_v.

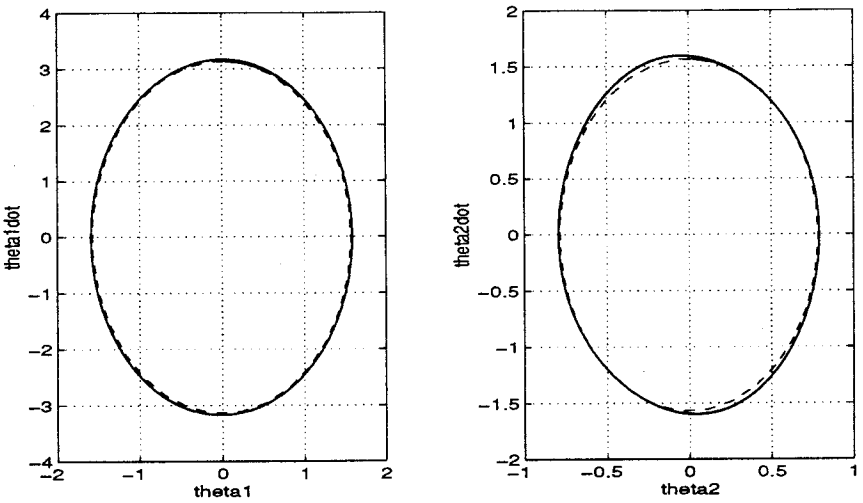

Fig. 2. $K_p = 24.0$, $K_v = 12.0$ and $\varepsilon = -0.1$.

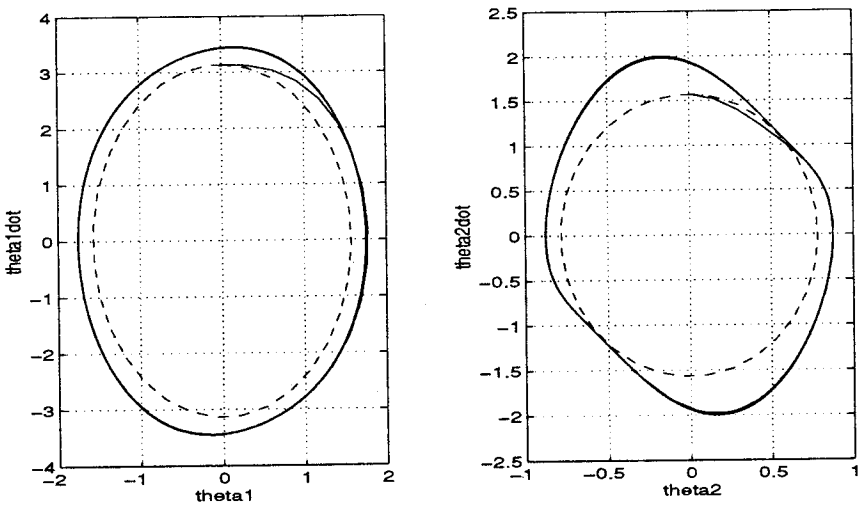

Fig. 3. $K_p = 24.0$, $K_v = 12.0$ and $\varepsilon = -0.5$.

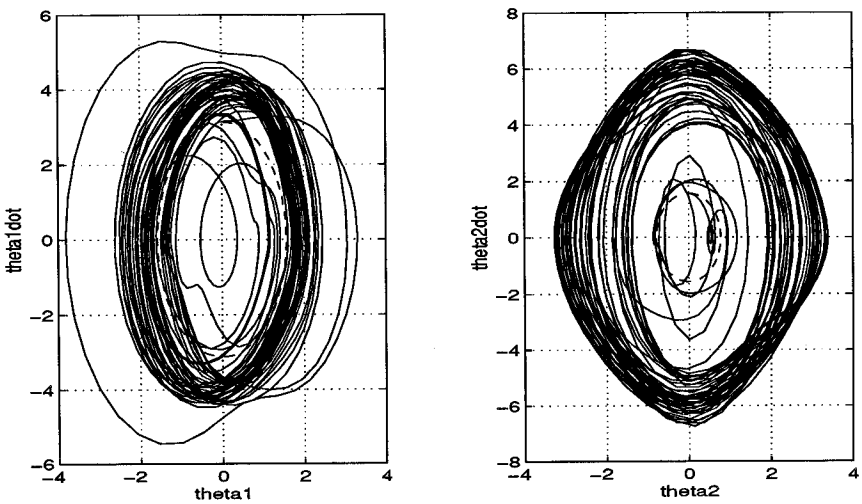

Fig. 4. $\varepsilon = -0.9$, $K_p = 25$ and $K_v = 4$.

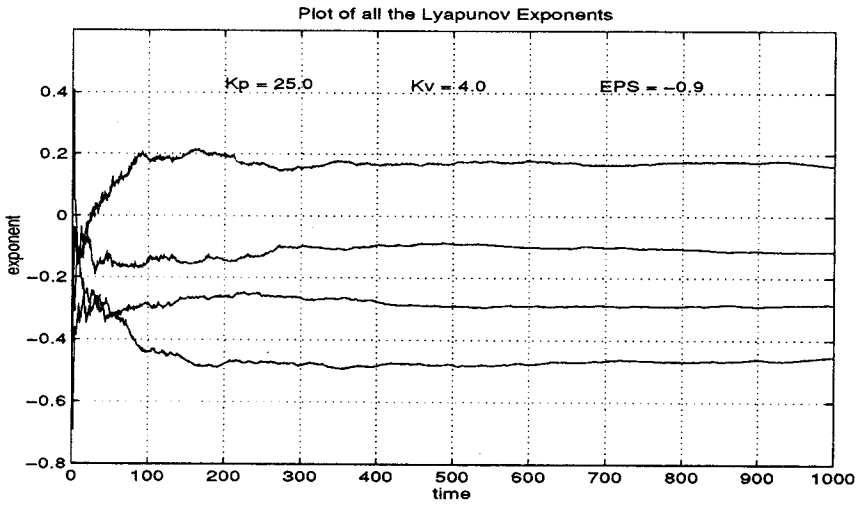

Fig. 5. Plot of all the Lyapunov exponents (Chaotic).

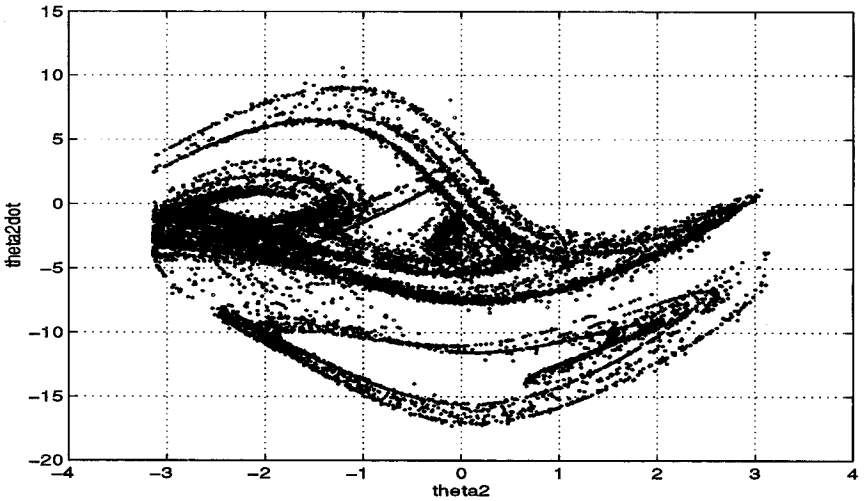

Fig. 6. Poincaré map, $\varepsilon = -0.85$, $K_p = 35.0$ and $K_v = 4.1$.

Figure 4 shows phase plots of a case when the performance is chaotic. The largest Lyapunov exponent (Fig. 5) is positive and three of them are negative.[2] This occurs in the case of a bad model, i.e. when the mismatch is large and for low values of gains. In Fig. 6, the Poincaré map is shown for $K_p = 35.0$, $K_v = 4.1$ and $\varepsilon = -0.85$.

A systematic search for chaotic parameters was done by stepping the parameters and computing the largest Lyapunov exponent. ε was stepped at intervals of 0.05 and K_v at intervals of 0.1 for a fixed value of K_p. Figures 7–10 show chaos maps for different values of the mismatch parameter ε. Chaotic behavior was seen only when the mismatch parameter, ε, was large (more than 0.6) and chaos was more easily seen for underestimations.

For overestimations, chaotic behavior was observed only for very small values of K_p and K_v. This can be explained by considering the closed-loop equation of the system for model-based control. Let us rewrite the equations of motion with the model based control law as,

$$\ddot{E} + \mathbf{M}^{-1}\hat{\mathbf{M}}K_v\dot{E} + \mathbf{M}^{-1}\hat{\mathbf{M}}K_pE = \mathbf{M}^{-1}\{[\mathbf{M} - \hat{\mathbf{M}}]\ddot{\theta}_d + [\mathbf{C} - \hat{\mathbf{C}}]\} \quad (15)$$

[2]The sum of all the Lyapunov exponents is negative since this is a dissipative system.

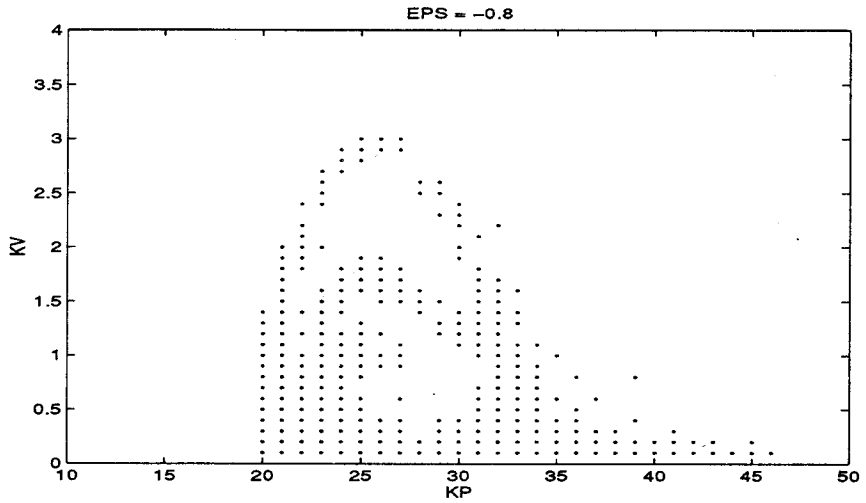

Fig. 7. Chaos map for model based control: $\varepsilon = -0.8$.

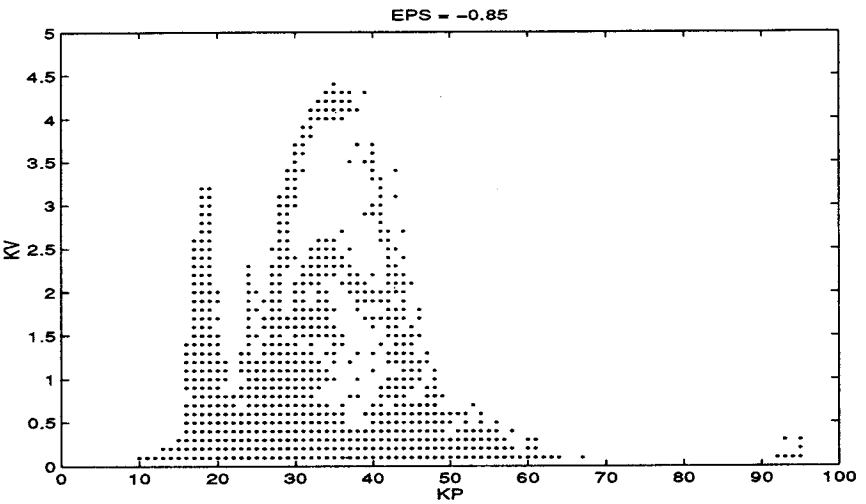

Fig. 8. Chaos map for model based control: $\varepsilon = -0.85$.

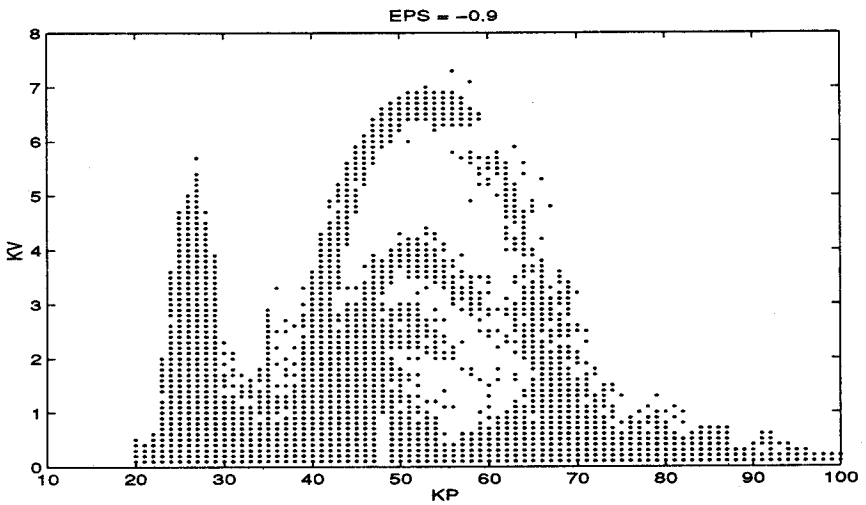

Fig. 9. Chaos map for model based control: $\varepsilon = -0.9$.

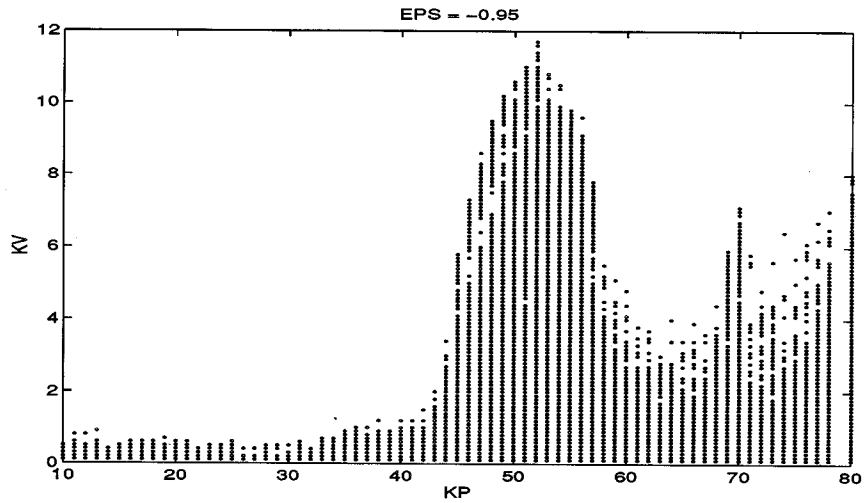

Fig. 10. Chaos map for model based control: $\varepsilon = -0.95$.

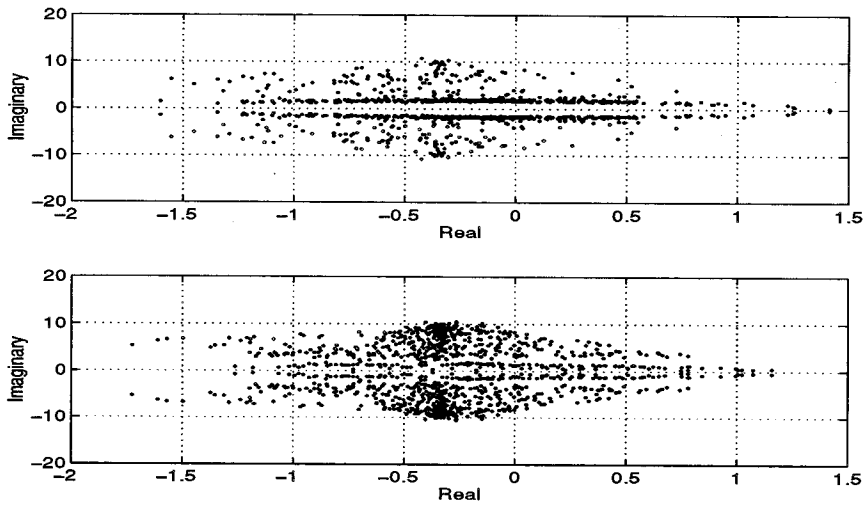

Fig. 11. Closed-loop poles for a chaotic case: $\varepsilon = -0.9$, $K_p = 50$ and $K_v = 6.5$.

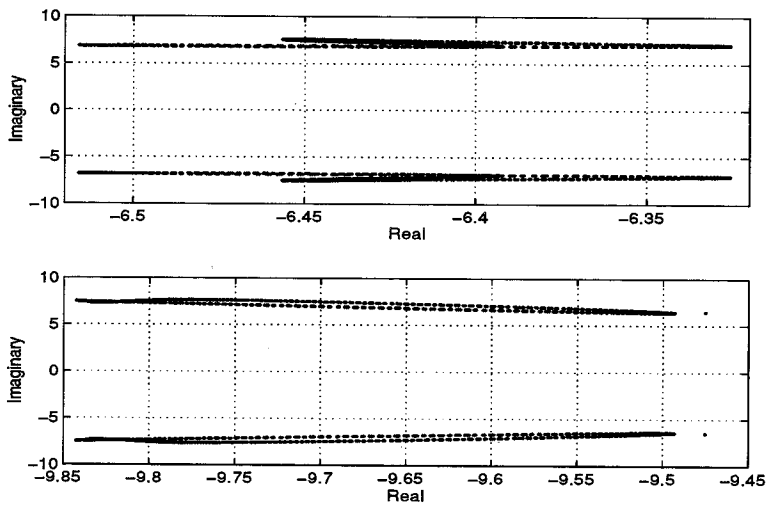

Fig. 12. Closed-loop poles for a non-chaotic case: $\varepsilon = 0.9$, $K_p = 50$ and $K_v = 6.5$.

It can be noted that if the parameters are not known exactly, the right side of the above equation does not cancel out but it is approximately in the order of the mismatch error. Examining the closed-loop gains of the system, i.e. $\mathbf{M}^{-1}\hat{\mathbf{M}}K_v$ and $\mathbf{M}^{-1}\hat{\mathbf{M}}K_p$, we note that the effective gains are scaled up if the model parameters are overestimated. This results in the closed-loop poles far to the left of the $j\omega$ axis. On the other hand, if the model parameters are underestimated, the effective gains become smaller than the actual set gains. This results in the closed-loop poles moving towards the $j\omega$ axis giving rise to chaotic behavior. This can be seen in Figs. 11 and 12 which show the location of the closed-loop poles for $K_p = 50$ and $K_v = 6.5$. The closed-loop poles of the linear system for $\varepsilon = 0$ are $-3.25 + 6.2799i$ and $-3.25 - 6.2799i$. As can be seen from Fig. 11 (chaotic case), the closed loop poles are nearer the $j\omega$ axis and sometimes go to the right half plane. In Fig. 12, when $\varepsilon > 0$, the poles are well to the left of $j\omega$ axis. The closed loop poles were calculated by numerically evaluating the eigenvalues of the instantaneous linearized state equations (13).

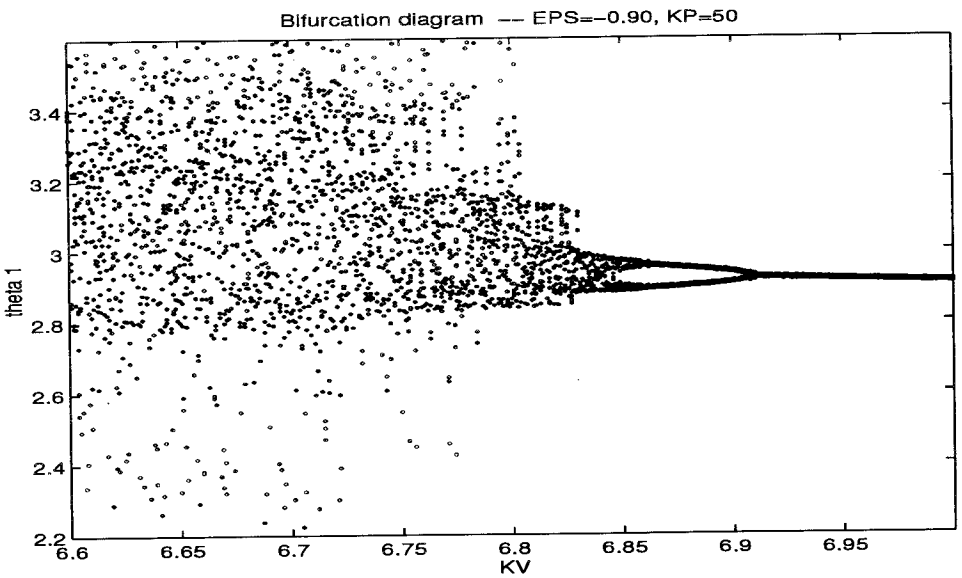

Fig. 13. Bifurcation diagram for θ_1 (model-based controller: $\varepsilon = -0.9$, $K_p = 50$).

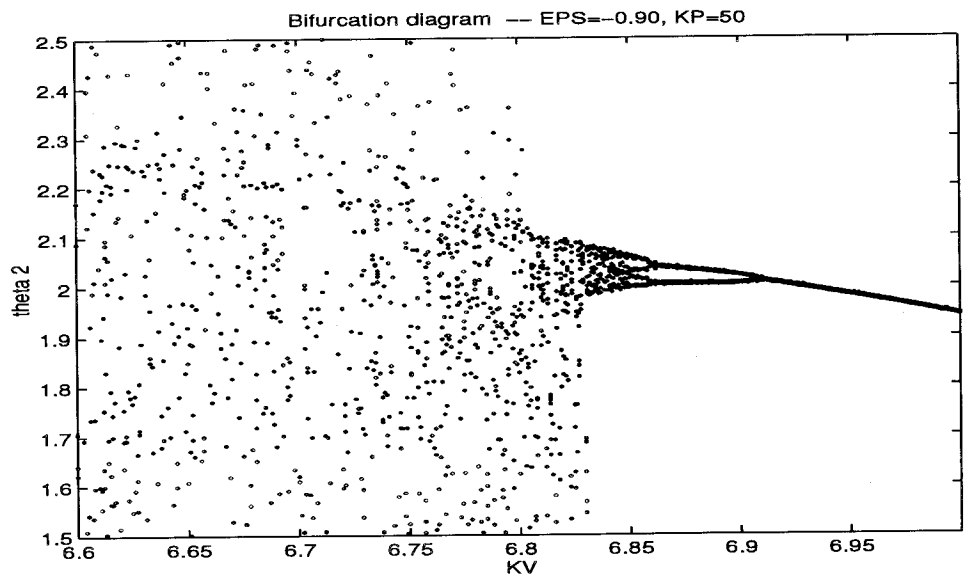

Fig. 14. Bifurcation diagram for θ_2 (model-based controller: $\varepsilon = -0.9$, $K_p = 50$).

Figures 13 and 14 show bifurcation diagrams for the model-based controller. A one to two bifurcation can be seen beyond which the system is chaotic. It should be noted that these diagrams were obtained by a brute force method and the figures are projections of the trajectory bifurcating in $\mathbb{R}^4$.

Figure 15 show the chaos map for the proportional and derivative controller which can be considered to be a special case of the model based controller with $\hat{\mathbf{M}}$ equal to the identity matrix and $\hat{\mathbf{C}}$ equal to zero. Again, it can be observed that chaos occurs for small values of the derivative gain and relatively large values of the proportional gain. Figures 16 and 17 show bifurcation diagrams for the proportional derivative controller. Clearly, bifurcation from one to two and two to four can be seen.

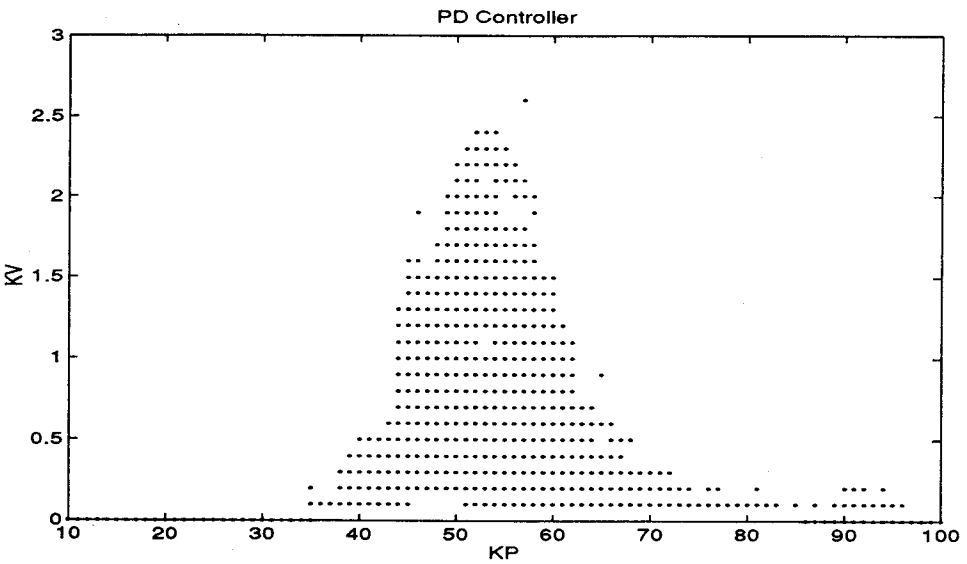

Fig. 15. Chaos map for PD control.

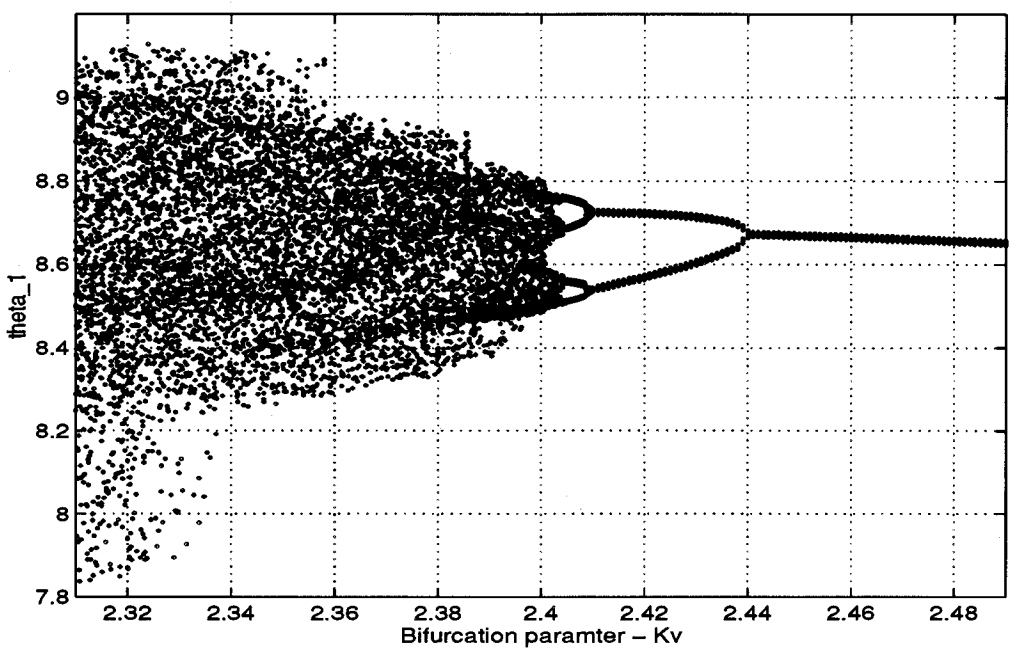

Fig. 16. Bifurcation diagram for θ_1 (PD controller: $K_p = 52$).

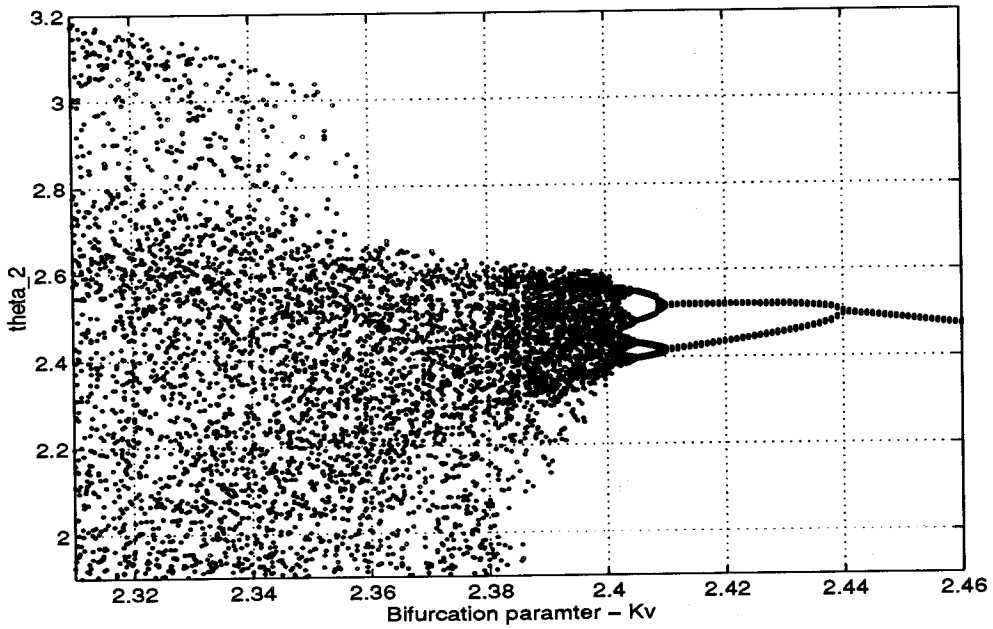

Fig. 17. Bifurcation diagram for θ_2 (PD controller: $K_p = 52$).

6. Conclusion

In this paper we have shown that the equations of a nonlinear feedback controller can exhibit chaos. These equations are very much different from those studied so far in literature. The trigonometric nonlinearities and coupling of the equations makes an analytical study difficult but a numerical study is feasible. From the careful numerical study we present the following major conclusions:

- Chaotic motions can be seen both for a simple PD controller and for a model-based controller with mismatch in model parameters. The existence of chaotic motions were verified by careful numerical simulations and by use of Lyapunov exponents.
- Chaotic motions occur for small values of the derivative gains and for large mismatch between the dynamic model and the actual robot parameters. Chaotic motions are only seen if the system is grossly underdamped. The chaotic motions are seen more easily for underestimated models. For overestimated models, chaotic motions are seen for extremely low values of controller gains. This can be explained by the observation that the effective closed loop gains for an overestimated model is larger than the proportional and derivative gains.
- Although, we have not been able to present analytical results, the numerical simulations suggest that one of the **possible** route to chaos may be through period doubling.

Although the range of controller gains, in particular the derivative gains, is far removed from critically damped (or overdamped) regime in any actual robot, this study, apart from being of mathematical interest, can give lower bounds on controller gains and can also help in obtaining conditions for better trajectory tracking in feedback controlled robots. This study also suggests that robustness results in robot control literature need a fresh look since the possibility of chaotic motions have not been considered by researchers.

References

Asada, H. & Slotline, J. J. E. [1986] *Robot Analysis and Control* (John Wiley and Sons).

Bühler, M. & Koditschek, D. E. [1990] "From stable to chaotic juggling: Theory, simulation, and experiments," *Proc. IEEE Int. Conf. Robotics and Automation* 1976–1981.

Bühler, M. & Koditschek, D. E. [1991] "Analysis of a simplified hopping robot," *Int. J. Robotics Research* **10**(6), 587–605.

Craig, John J. [1989] *Introduction to Robotics: Mechanics and Control* (Addison-Wesley Publishing Company).

Craig, John J. [1988] *Adaptive Control of Mechanical Manipulators* (Addison-Wesley Publishing Company).

Dullin, R. H. [1994] "Melnikov's method applied to the

double pendulum," *Zeitschrift für Physik* **B93**, 521–528.

Gordon, M. K. & Shampine, L. F. [1975] *Computer Solutions of Ordinary Differential Equations: The Initial Value Problem* (W. H. Freeman & Co.)

Khosla, P. K. [1986] "Real-time control and identification of direct-drive manipulators," Ph.D. Thesis, Dept. of Electrical and Computer Eng., Carnegie Mellon University, USA.

Levien, R. B. & Tan, S. M. [1993] "Double pendulum: An experiment in chaos," *Am. J. Phys.* **61**(11), 1038–1044.

Mahout, V., Lopez, P., Carcassés, J. P. & Mira, C. [1992] "Complex responses (chaotic) of a two-revolute joints robot for periodical torque inputs, *IFToMM-jc Int. Symp. Theor. Machines and Mechanisms* (Nagoya, Japan).

Mahout, V., Lopez, P., Carcassés, J. P. & Mira, C. [1993] "Complex behaviors of a two-revolute joints robot: Harmonic, subharmonic, higher harmonic, fractional harmonic, chaotic responses," *Int. Conf. System, Man and Cybernetics* **5**, 201–205.

M'Closkey, R. T. & Burdick, J. W. [1993] "Periodic motions of a hopping robot with vertical and forward motion," *Int. J. Robotics Research* **12**(3), 197–218.

Moon, F. C. [1987] *Chaotic Vibrations* (John Wiley and Sons).

Parker, T. S. & Chua, L. O. [1989] *Practical Numerical Algorithms for Chaotic Systems* (Springer-Verlag).

Richter, P. H. & Scholz, H. J. [1983] "Chaos in classical mechanics: The double pendulum," in *Stochastic Phenomena and Chaotic Behavior in Complex Systems* ed. Schuster, P. (Springer).

Shinbrot, T., Grebogi, C., Wisdom, J. & Yorke, J. A. [1992] "Chaos in a double pendulum," *Am. J. Phys.* **60**(6), 491–499.

Spong, M. W. & Vidyasagar, M. [1989] *Robot Dynamics and Control* (John Wiley and Sons).

Streit, D. A., Krousgrill, C. M. & Bajaj, A. K. [1986] "A preliminary investigation of the dynamic stability of flexible manipulators performing repetitive tasks," *Trans. ASME: J. Dynamic Systems, Measurement and Control* **108**, 206–214.

Streit, D. A., Krousgrill, C. M. & Bajaj, A. K. [1989] "Nonlinear response of flexible robotic manipulators performing repetitive tasks," *Trans. ASME: J. Dynamic Systems, Measurement and Control* **111**, 470–480.

Streit, D. A., Krousgrill, C. M. & Bajaj, A. K. [1988] "Combination parametric resonance leading to periodic and chaotic response in two-degree-of-freedom systems with quadratic non-linearities," *J. Sound and Vibration* **124**(2), 470–480.

User's Manual IMSL Math/Library [1989].

Vakakis, A. F. & Burdick, J. W. [1990] "Chaotic motions in the dynamics of a hopping robot," *Proc. IEEE Int. Conf. Robotics and Automation* 1464–1469.

Vakakis, A. F., Burdick, J. W. & Caughey, T. K. [1991] "An interesting strange attractor in the dynamics of a hopping robot," *Int. J. Robotics Research* **10**(6), 606–618.

Wolf, A., Swift, J. B. Swinney, H. A. & Vastano, J. A. [1985] "Determining Lyapunov exponents from a time series," *Physica* **D16**, 285–317.